

Supporting Information

Officinalins A and B, a pair of C₂₃ Terpenoid Epimers with a Tetracyclic 6/7/5/5 System from *Salvia officinalis*

Ling-Nan Li, Xiao-Qin Liu, Dong-Rong Zhu, Chen Chen, Yao-Lan Lin, Wen-Li Wang, Li Zhu, Jian-Guang Luo,* and Ling-Yi Kong*

Jiangsu Key Laboratory of Bioactive Natural Product Research and State Key Laboratory of Natural Medicines, China Pharmaceutical University, 24 Tong Jia Xiang, Nanjing 210009, People's Republic of China.

* Corresponding Authors. Tel/Fax: +86-25-83271405;

E-mail: cpu_lykong@126.com (Ling-Yi Kong); luojg@cpu.edu.cn (Jian-Guang Luo).

List of contents

1. Experimental section

1.1 General experimental procedures

1.2 Plant material

1.3 Extraction and purification

1.4 Quantum-chemical electronic circular dichroism (ECD) calculations

1.5 The optimized conformations of A and B

1.6 NO inhibitory activity assay

2. Fig. S1 Overview of all reported natural C₂₃ terpenoids structures.

3. Table S1 ¹H (600 MHz) and ¹³C (150 MHz) NMR data of **2** in DMSO-*d*₆.

4. Table S2 Five conformers of A were obtained after the optimization.

5. Table S3 Four conformers of B were obtained after the optimization.

6. Fig. S2 Two minimized conformers (A and B).

7. Table S4 Inhibitory effects on NO production in LPS-induced RAW264.7 cells of compounds **1-3**.

8. Fig. S3 Cell viability (A) and NO Inhibition rate (B) in LPS stimulated RAW264.7 cells of **1**. Data shown are the mean ± SEM (n=3).

9. Spectroscopic data section

Fig. S4 ¹H NMR (600 MHz) spectrum of officinalin A (**1**) in CDCl₃

Fig. S5 ¹³C NMR (150 MHz) spectrum of officinalin A (**1**) in CDCl₃

Fig. S6 ¹H-¹H COSY spectrum of officinalin A (**1**) in CDCl₃

Fig. S7 HSQC spectrum of officinalin A (**1**) in CDCl₃

Fig. S8 HMBC spectrum of officinalin A (**1**) in CDCl₃

Fig. S9 ROESY spectrum of officinalin A (**1**) in CDCl₃

Fig. S10 HRESIMS spectrum of officinalin A (**1**) in MeOH

Fig. S11 CD spectrum of officinalin A (**1**) in MeCN

Fig. S12 ¹H NMR (600 MHz) spectrum of officinalin B (**2**) in CDCl₃

Fig. S13 ¹³C NMR (150 MHz) spectrum of officinalin B (**2**) in CDCl₃

Fig. S14 ¹H-¹H COSY spectrum of officinalin B (**2**) in CDCl₃

- Fig. S15** HSQC spectrum of officinalin B (**2**) in CDCl₃
- Fig. S16** HMBC spectrum of officinalin B (**2**) in CDCl₃
- Fig. S17** ROESY spectrum of officinalin B (**2**) in CDCl₃
- Fig. S18** ¹H NMR (600 MHz) spectrum of officinalin B (**2**) in DMSO-*d*₆
- Fig. S19** ¹³C NMR (150 MHz) spectrum of officinalin B (**2**) in DMSO-*d*₆
- Fig. S20** HSQC spectrum of officinalin B (**2**) in DMSO-*d*₆
- Fig. S21** HMBC spectrum of officinalin B (**2**) in DMSO-*d*₆
- Fig. S22** ROESY spectrum of officinalin B (**2**) in DMSO-*d*₆
- Fig. S23** HRESIMS spectrum of officinalin B (**2**) in MeOH
- Fig. S24** CD spectrum of officinalin B (**2**) in MeCN
- Fig. S25** ¹H NMR (600 MHz) spectrum of compound **3** in CDCl₃
- Fig. S26** ¹³C NMR (150 MHz) spectrum of compound **3** in CDCl₃

1. Experimental section

1.1 General experimental procedures

A JASCO J-810 spectrometer (Jasco, Tokyo, Japan) was employed to record the CD spectra. Optical rotations were conducted on a JASCO P-1020 polarimeter (Jasco, Tokyo, Japan) at 20 °C. The UV/vis spectra were determined with a UV-2450 UV/vis spectrophotometer (Shimadzu, Tokyo, Japan). A Bruker Avance-600 NMR instrument (Bruker, Karlsruhe, Germany) was acquired in CDCl₃ or DMSO-*d*₆. Chemical shift values (δ) were expressed in parts per million (ppm) and coupling constants in Hertz. All the accurate mass experiments were performed on an Agilent 6520B UPLC-Q-TOF instrument (Agilent Technologies, Santa Clara, CA, USA). Silica gel (200-300 mesh; Qingdao Haiyang Chemical Co., Ltd, Qingdao, China), and RP-C18 (40-63 μ m, Fuji, Japan) were employed in the column chromatography. Preparative HPLC (Pre-HPLC) was conducted on a Shimadzu LC-8A system, which was equipped with a Shim-pack reversed-phase (RP-C₁₈) column chromatography (CC) (20 mm \times 200 mm, i.d., 10 μ m), by a binary channel UV detector at 230 nm.

All reagents and solvents used in current work were provided from commercial suppliers resources (Jiangsu Hanbang Sci. & Tech. Co., Ltd., China). Fetal bovine serum (FBS) and dulbecco's modified Eagle's medium (DMEM) were supplied by Invitrogen (Carlsbad, CA, USA). Streptomycin, penicillin, trypsin, LPS, 3-(4,5-dimethylthiazol-2-yl)-2,5-diphenyltetrazolium bromide (MTT) and dimethyl sulphoxide (DMSO) were provided from Sigma Chemical Co., Ltd. (St. Louis, MO, USA). All antibodies were supplied by Cell Signaling Technology (Beverly, MA, USA). PVDF membrane was supplied by Bio-Rad Laboratories (Hercules, CA, USA).

1.2 Plant material

Salvia officinalis leaves were obtained from Xinhe Spices Corporation (Haikou, China), in February 2017. A voucher specimen (No. 2017-SO) was deposited in the Department of Natural Medicinal Chemistry, China Pharmaceutical University. The plant specimens were identified by an expert from China Pharmaceutical University

(Professor Min-Jian Qin, Nanjing, China).

1.3 Extraction and purification

The air-dried leaves of *S. officinalis* (5.0 kg) were smashed and exhaustively extracted with 95 % ethanol for three times (each for 2 h) under reflux. The obtained crude extract (485 g) was suspended in distilled water and successively partitioned with n-hexane (Hex), dichloromethane (DCM) and ethyl acetate (EA) after the solvent was removed under reduced pressure. The Hex extract (123 g) was further fractionated onto a silica gel CC with a gradient of PE-EA (100:1-1:1, v/v) as the mobile phase to yield six fractions (A-F). Fr.C (27.7 g) was loaded on a Sephadex LH-20 column and eluted with acetone to yield Fr.C1–C8. Further purification of Fr.C3 was carried out using RP-C₁₈ CC to yield Fr.C3-1–C3-6, eluted with MeOH-H₂O (50:50-100:0, v/v). Subsequently, Fr.C3-4 were purified using Pre-HPLC (MeOH:H₂O = 80:20, v/v) to yield **1** (1.2 mg), **2** (4.3 mg). Fr.C5 (12.5 g) was further loaded on RP-C₁₈ CC to yield Fr.C5-1–C5-6. Fr.C5-4 was purified using Pre-HPLC (MeOH:H₂O = 85:15, v/v) to yield **3** (6.2 mg).

Officinalin A (1): faint yellowish amorphous powder; $[\alpha]_{25}^{D} 9.5$ (*c* 0.1, MeOH); HRESIMS: m/z 375.2529 $[M + H]^+$ (C₂₃H₃₅O₄ calcd for 375.2530); UV (MeOH) $\lambda_{\max}(\log \epsilon)$ 207.50 (1.48) nm; ¹H and ¹³C NMR (in CDCl₃): see Table 1.

Officinalin B (2): faint yellowish amorphous powder; $[\alpha]_{25}^{D} -10.5$ (*c* 0.1, MeOH); HRESIMS m/z 375.2531 $[M + H]^+$ (C₂₃H₃₅O₄ calcd for 375.2530); UV (MeOH) $\lambda_{\max}(\log \epsilon)$ 209.50 (1.64) nm; ¹H and ¹³C NMR (in CDCl₃): see Table 1; ¹H and ¹³C NMR ((in DMSO-*d*₆): see Table S1.

Compound 3 (deacetoxynemorone): yellow gum; ESI-MS m/z 331.42 $[M+H]^+$; ¹H NMR (CDCl₃, 600 MHz): δ_{H} 0.75 (3H, s, H-19), 0.97 (3H, s, H-18), 1.19 (3H, d, *J* = 7.1 Hz, H-16), 1.21 (3H, d, *J* = 7.1 Hz, H-17), 1.24 (1H, td, *J* = 13.4, 4.4 Hz, H-1 β), 1.31 (1H, td, *J* = 13.4, 4.4 Hz, H-3 α), 1.40 (1H, d, *J* = 12.4 Hz, H-5), 1.55 (1H, br d, *J* = 13.5 Hz, H-3 β), 1.69 (1H, m, H-6 α), 1.74 (1H, m, H-2 α), 1.87 (1H, dd, *J* = 13.5, 6.5 Hz, H-6 β), 1.98 (1H, qt, *J* = 14.3, 3.8 Hz, H-2 β), 2.37 (1H, m, H-7 α), 2.83 (1H, dd,

$J = 20.8, 4.8$ Hz, H-7 β), 3.06 (1H, br d, $J = 13.6$ Hz, H-1 α), 3.15 (1H, sept, $J = 7.1$ Hz, H-15), 6.95 (1H, s, OH), 10.1 (1H, s, H-20); ^{13}C NMR (CDCl_3 , 150 MHz): δ_{C} 16.7 (C-6), 19.2 (C-2), 19.9 (C-17), 20.0 (C-16), 22.8 (C-19), 24.3 (C-15), 26.4 (C-7), 31.6 (C-18), 32.5 (C-1), 33.8 (C-4), 40.9 (C-3), 51.3 (C-10), 54.5 (C-5), 125.1 (C-13), 141.0 (C-9), 149.5 (C-8), 150.5 (C-12), 182.6 (C-11), 186.9 (C-14), 203.5 (C-20)。

1.4 Quantum-chemical electronic circular dichroism (ECD) calculations

Monte Carlo conformational searches were carried out by means of the Spartan's 10 software using MMFF94 molecular mechanics force-field. The conformers with Boltzmann-population of over 5% were chosen for ECD calculations, and then the conformers were initially optimized at B3LYP/6-31+G (d,p) level using the CPCM polarizable conductor calculation model. The theoretical calculation of ECD was conducted using TD-DFT at the B3LYP/6-31+G (d,p) level for all conformers of compounds **1** and **2**. Rotatory strengths for a total of 30 excited states were calculated. ECD spectra were generated using the program SpecDis 1.6 (University of Würzburg, Würzburg, Germany) and GraphPad Prism 5 (University of California San Diego, USA) from dipole-length rotational strengths by applying Gaussian band shapes with $\sigma = 0.3$ eV.

1.5 The optimized conformations of A and B.

The optimized conformation of A: Five conformations (A1~A5) were obtained by the systematic searches (Table S2). The distances between OH-10 and OH-13, between H-7 α and H-23, between H-7 β and H-11, and between H-7 β and H-16 β were 6.5 Å, 7.2 Å, 5.8 Å, and 6.2 Å, respectively, not in agreement with the correlation between OH-10 and OH-13, between H-7 α and H-23, between H-7 β and H-11, and between H-7 β and H-16 β in the ROESY spectra of compound **1**.

The optimized conformation of B: By using same method that for B, four conformations (B1~B4) were obtained after optimization (Table S3). This is also supported by ROESY experiment of compound **2**, in which obvious cross peaks were observed between OH-10 and OH-13, between H-7 α and H-23, between H-7 β and H-

11, and between H-7 β and H-16 β .

1.6 NO inhibitory activity assay

1.6.1 Cell culture

The mouse macrophage cell line RAW264.7 was purchased from the Cell Bank of the Shanghai Institute of Cell Biology and Biochemistry, Chinese Academy of Sciences. Cells were maintained in DMEM containing 10% FBS, streptomycin (100 $\mu\text{g}/\text{mL}$) and penicillin (100 U/mL) at 37 °C in an incubator containing 5% CO₂.

1.6.2 Cell viability assay

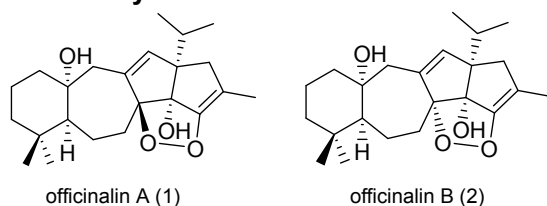
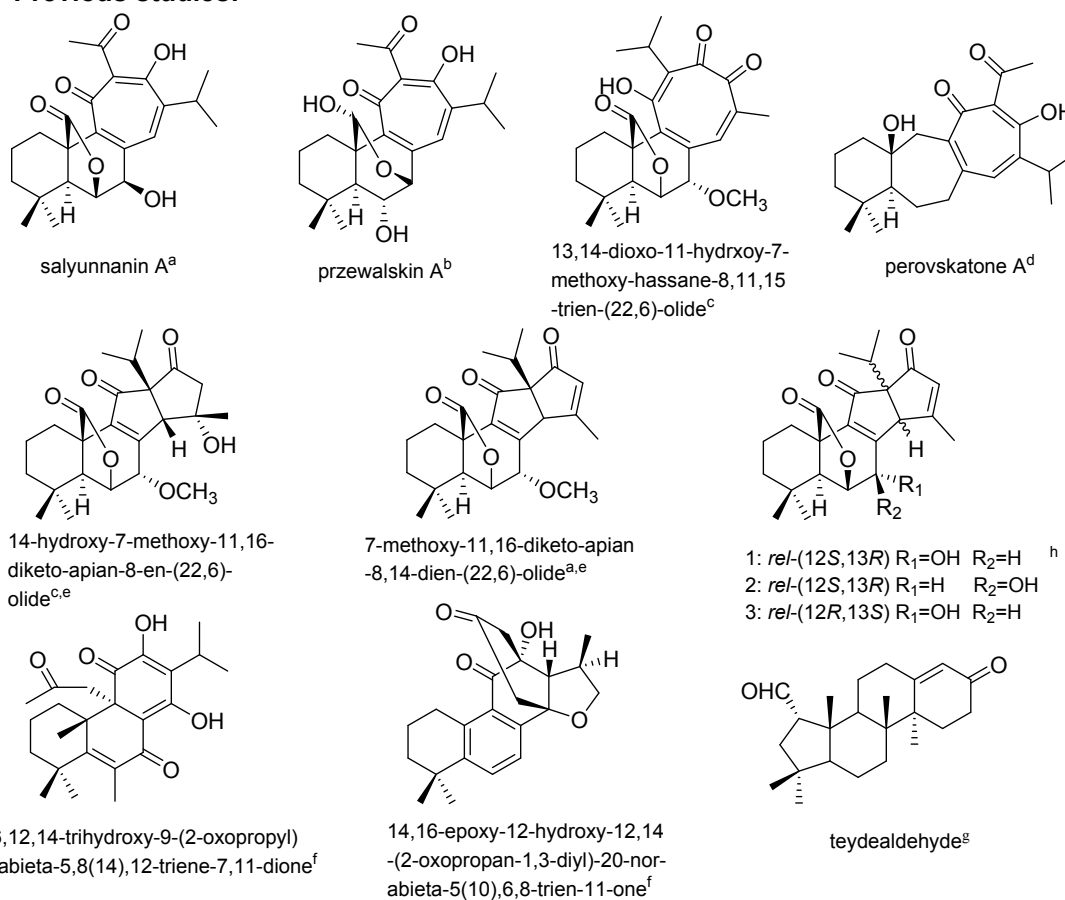
Cell viability was determined by MTT assay. Briefly, RAW264.7 cells were seeded at a density of 5×10^4 cells/mL into 96-well plates and incubated for 18 h. Subsequently, cells were challenged by five concentrations of samples, followed by 1 h incubation, and cells were then exposed to LPS (1 $\mu\text{g}/\text{mL}$) for another 18 h. Subsequently, MTT solution (0.5 mg/mL) was added into each well, and the mixture was then incubated at 37 °C for 4 h. After formazan was fully dissolved in DMSO, the absorption values at 570 nm (reference, 630 nm) were determined using a microplate reader (Molecular Devices, USA).

1.6.3 NO release assay

NO production was measured in cell culture supernatants with the Griess reagent according to the level of nitrite accumulation. Briefly, RAW264.7 cells were seeded at a density of 6×10^5 cells/mL into 96-well plates and pretreated with test samples for 1 h. Subsequently, cells were exposed to 1 $\mu\text{g}/\text{mL}$ LPS for 18 h. Next, 50 μL culture supernatant and 50 μL Griess reagent were mixed. After 10 min, the absorbance values at a wavelength of 540nm were recorded by a microplate reader. And nitrite contents were measured by sodium nitrate as a standard. N^G-Monomethyl-L-arginine (L-NMMA) served as a positive control in the experiments.

1.6.4 Western blotting analysis

After exposed to LPS (1 $\mu\text{g}/\text{mL}$), cells were harvested and lysed by 1% radio-immunoprecipitation assay (RIPA) (Amresco, Solon, OH, USA) buffer. The cell lysates were centrifuged, supernatant was collected, and the protein content was measured by the BCA protein assay. Equal amounts of total proteins were subjected to SDS-PAGE and then electro-transferred onto PVDF membrane. The membranes were blocked using TBST buffer, containing 5% skimmed milk at 25 °C for 2 h, incubated with primary antibodies for 12 h at 4 °C, and then probed with secondary antibody at ambient temperature. The immunoreactive bands were visualized by ECL reagents, and imaging densitometry was quantified using a ChemiDOC XRS+ system (Bio-Rad Laboratories).

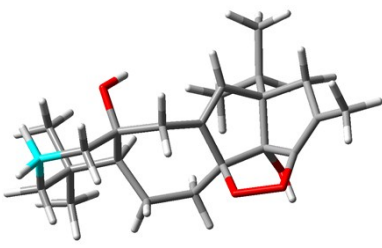
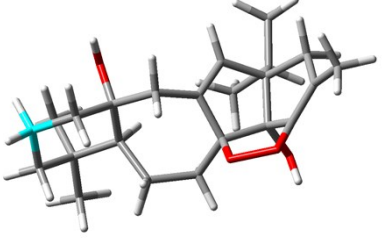
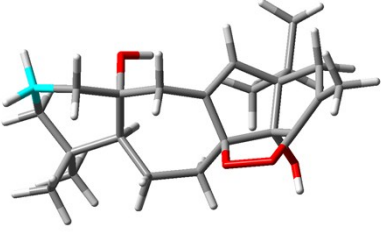
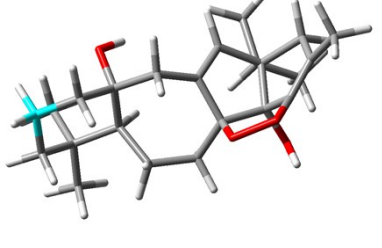
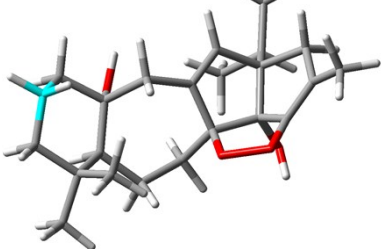
This study:**Previous studies:****Fig. S1** Overview of all reported natural C₂₃ terpenoids structures.**references**

- (a) C. Y. Wu, Y. Liao, Z. G. Yang, X. W. Yang, X. L. Shen, R. T. Li and G. Xu, *Phytochemistry*, 2014, **106**, 171-177. (b) G. Xu, A. J. Hou, R. R. Wang, G. Y. Liang, Y. T. Zheng, Z. Y. Liu, X. L. Li, Y. Zhao, S. X. Huang, L. Y. Peng and Q. S. Zhao, *Org. Lett.*, 2006, **8**, 4453-4456. (c) J. G. Luis, E. H. Lahlou and L. S. Andres, *Tetrahedron*, 1996, **52**, 12309-12312. (d) Z. Y. Jiang, C. G. Huang, H. B. Xiong, K. Tian, W. X. Liu, Q. F. Hu, H. B. Wang, G. Y. Yang and X. Z. Huang, *Tetrahedron Lett.*, 2013, **54**, 3886 - 3888. (e) J. G. Luis, E. H. Lahlou, L. S. Andres, G. H. N. Sood and M. M. Ripoll, *Tetrahedron Lett.*, 1996, **37**, 4213-4216. (f) C. Gaspar-Marques, M. F. Simoes and B. Rodriguez, *J. Nat. Prod.*, 2005, **68**, 1408-1411. (g) B. M. Fraga, C. E. Diaz and L. J. Amador, *Tetrahedron Lett.*, 2013, **37**, 4337-4338. (h) K. Miura, H. Kikuzaki and N. Nakatani, *Phytochemistry*, 2001, **58**, 1171-1175.

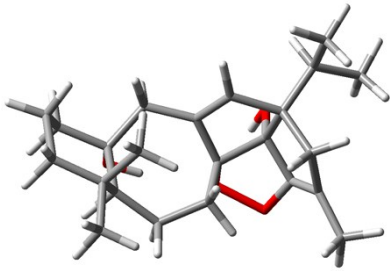
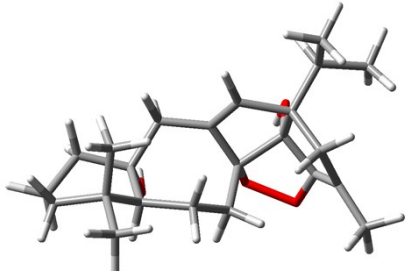
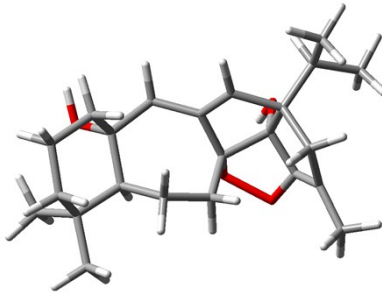
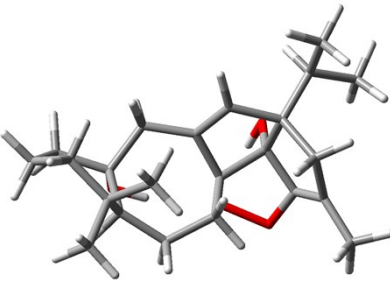
3. Table S1 ^1H (600 MHz) and ^{13}C (150 MHz) NMR data of **2** in $\text{DMSO-}d_6$.

Position	2			
	δ_{H} (J in Hz)	δ_{C}	HMBC	ROESY
1 α	1.66 m	41.7		OH-10
1 β	1.46 m		C-2, C-3, C-22	
2 α	1.35 m	17.7	C-5	
2 β	1.67 m			
3 α	1.45 m	41.6	C-2, C-1	Me-20
3 β	1.11 m		C-2, C-1	
4		33.9		
5	1.02 dd (1.7, 10.9)	55.2	C-4, C-6, C-7, C-20, C-21	H-7 α
6 α	1.89 m	24.4	C-5	H-7 α
6 β	1.69 m		C-4	H-7 β
7 α	2.50 dd (14.2, 5.6)	28.6	C-5, C-6, C-9, C-8	H-5, H-6 α , H-22 α , OH-13
7 β	1.90 t (12.4)		C-9	H-6 β , H-11, H-16 β
8		90.6		
9		144.		
10		9		
11		71.5		
11	5.91 s	136.	C-8, C-9, C-12, C-13, C-17	H-7 β
12		3		
12		53.6		
13		83.6		
14		174.		
14		0		
15		104.		
15		3		
16 α	1.84 d (13.9)	34.4	C-11, C-12, C-15	Me-19
16 β	1.68 d (13.9)		C-11, C-12, C-15	H-7 β
17	1.92 sept (7.0)	28.5	C-11, C-12, C-16, C-18, C-19	
18	0.70 d (7.0)	16.5	C-12, C-17, C-19	
19	0.82 d (7.0)	17.4	C-12, C-17, C-18,	H-16 α , OH-13
20	0.78 s	21.4	C-3, C-4, C-5, C-21	H-3 α , OH-10
21	0.83 s	32.3	C-3, C-4, C-5, C-20	
22 α	1.70 d (13.1)	49.9	C-8, C-9, C-10	H-7 α , OH-13
22 β	1.72 d (13.1)		C-8, C-9, C-10	
23	1.39 s	25.2	C-14, C-15, C-16	
OH-10	5.43 s		C-1, C-5, C-10, C-22	H-1 α , Me-20, OH-13
OH-13	7.07 s		C-8, C-12, C-13, C-14	H-7 α , H-22 α , OH-10, Me-19

4. Table S2 Five conformers of **A** were obtained after the optimization. Gibbs free energies and equilibrium populations of low-energy conformers at B3LYP/6-31+G (d,p) level.

no	conformer	ΔG (kJ/mol)	Population (%)
A1		0.00	86.90
A2		1.41	8.00
A3		2.25	3.00
A4		2.46	1.40
A5		2.87	0.70

5. Table S3 Four conformers of **B** were obtained after the optimization. Gibbs free energies and equilibrium populations of low-energy conformers at B3LYP/6-31+G (d,p) level

no	conformer	ΔG (kJ/mol)	Population (%)
B1		0.00	99.18
B2		0.00465	0.70
B3		0.01031	0.08
B4		0.0111	0.04

6. Two conformers (**A**, 5*S**,8*S**,10*R**,12*S**,13*R**; **B**, 5*S**,8*R**,10*R**,12*S**,13*R**) are shown in Figure S1. A systematic conformational analysis was performed for **A** and **B** using MMFF94 force-field calculations.

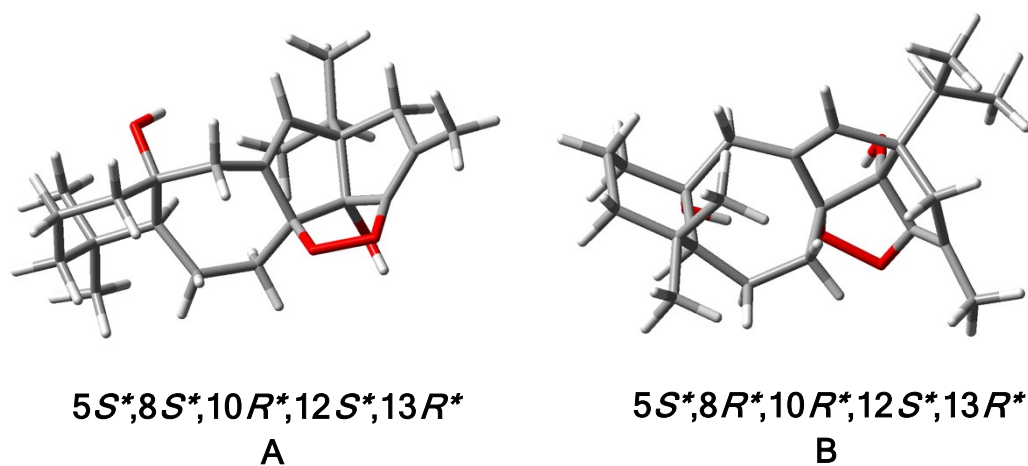


Fig. S2 Two minimized conformers after the optimization (**A** and **B**).

7. **Table S4** Inhibitory effects on NO production in LPS-induced RAW264.7 cells of compounds **1-3**.

Compounds	IC ₅₀ (μM) ^a
officinalin A (1)	2.02 ± 0.87
officinalin B (2)	6.35 ± 1.36
deacetoxynemorone (3)	19.70 ± 1.08
L-NMMA ^b	35.38 ± 0.75

^a mean ± SD of the three replicates.

^b N^G-Monomethyl-L-arginine as a positive control.

8.

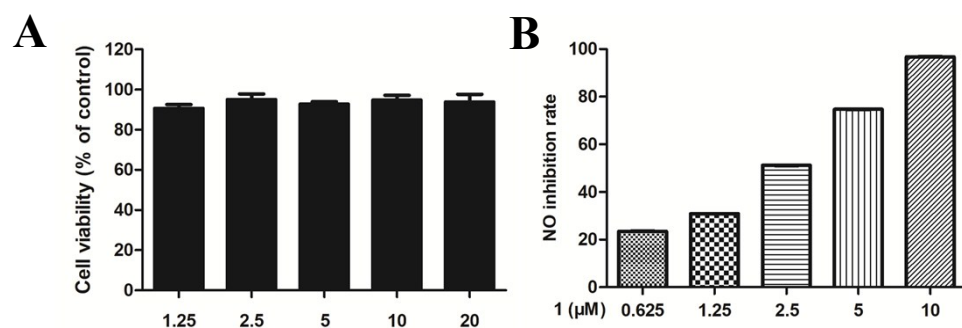


Fig. S2 Cell viability (**A**) and NO Inhibition rate (**B**) in LPS stimulated RAW264.7 cells of **1**. Data shown are the mean ± SEM (n=3).

9. Spectroscopic data section

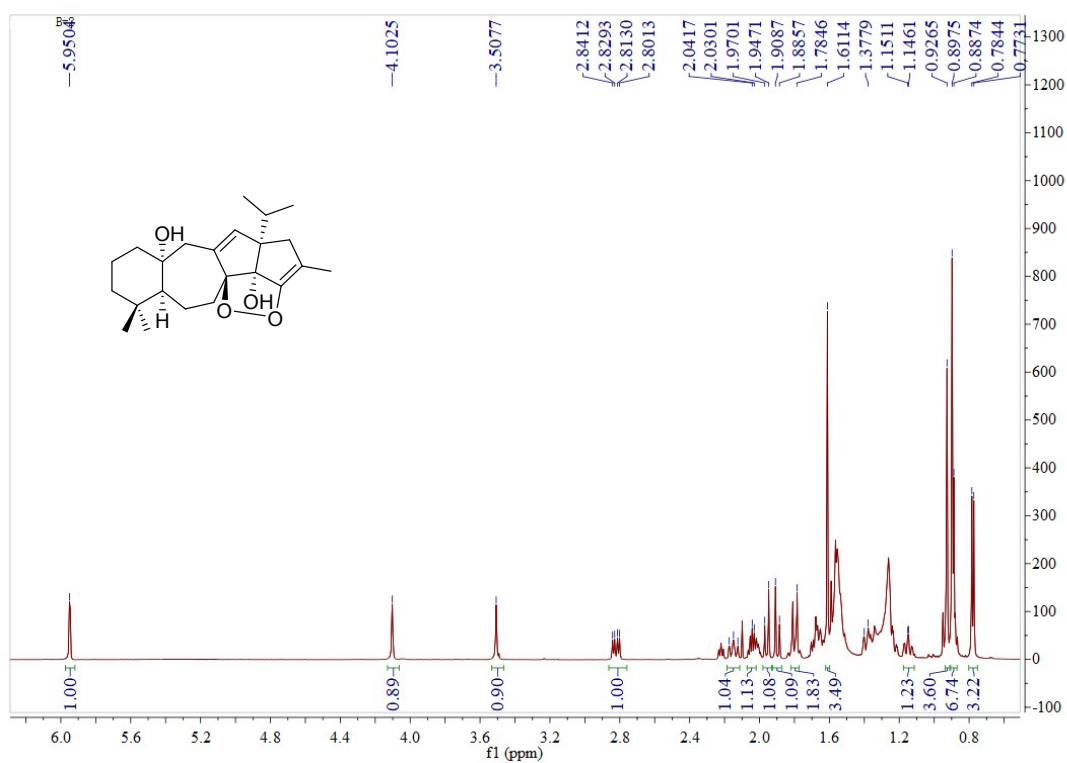


Fig. S4 ¹H NMR (600 MHz) spectrum of officinalin A (1) in CDCl₃

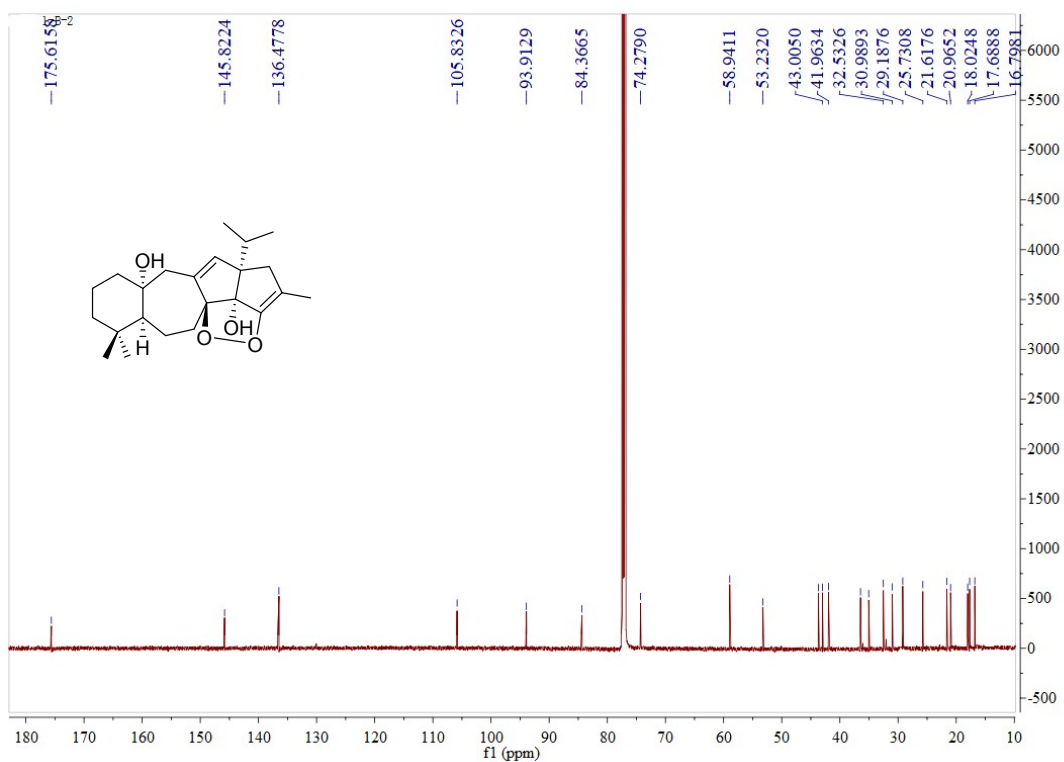


Fig. S5 ¹³C NMR (150 MHz) spectrum of officinalin A (1) in CDCl₃

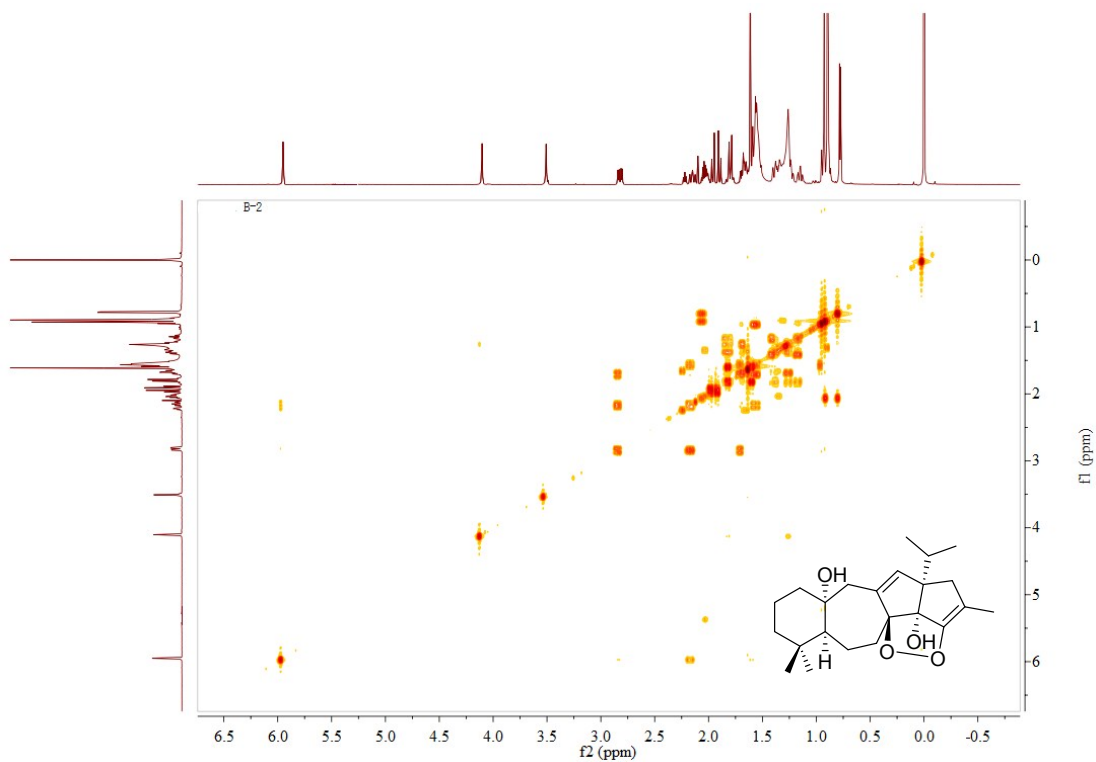


Fig. S6 ^1H - ^1H COSY spectrum of officinalin A (**1**) in CDCl_3

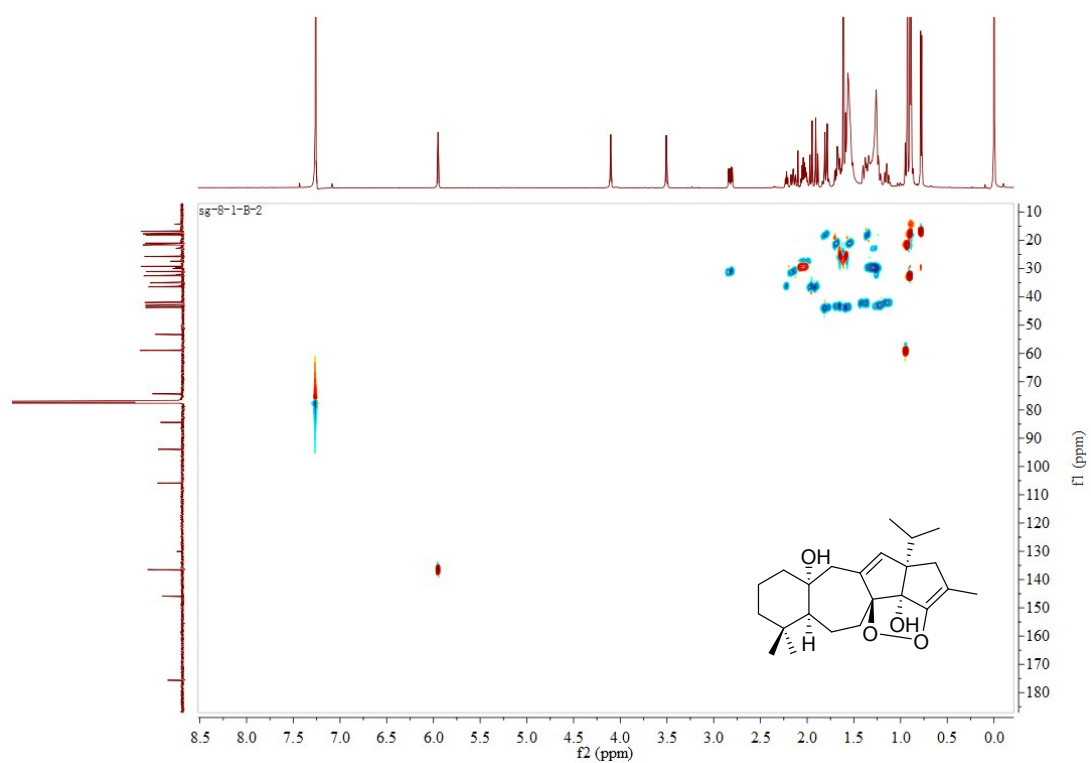


Fig.S7 HSQC spectrum of officinalin A (**1**) in CDCl_3

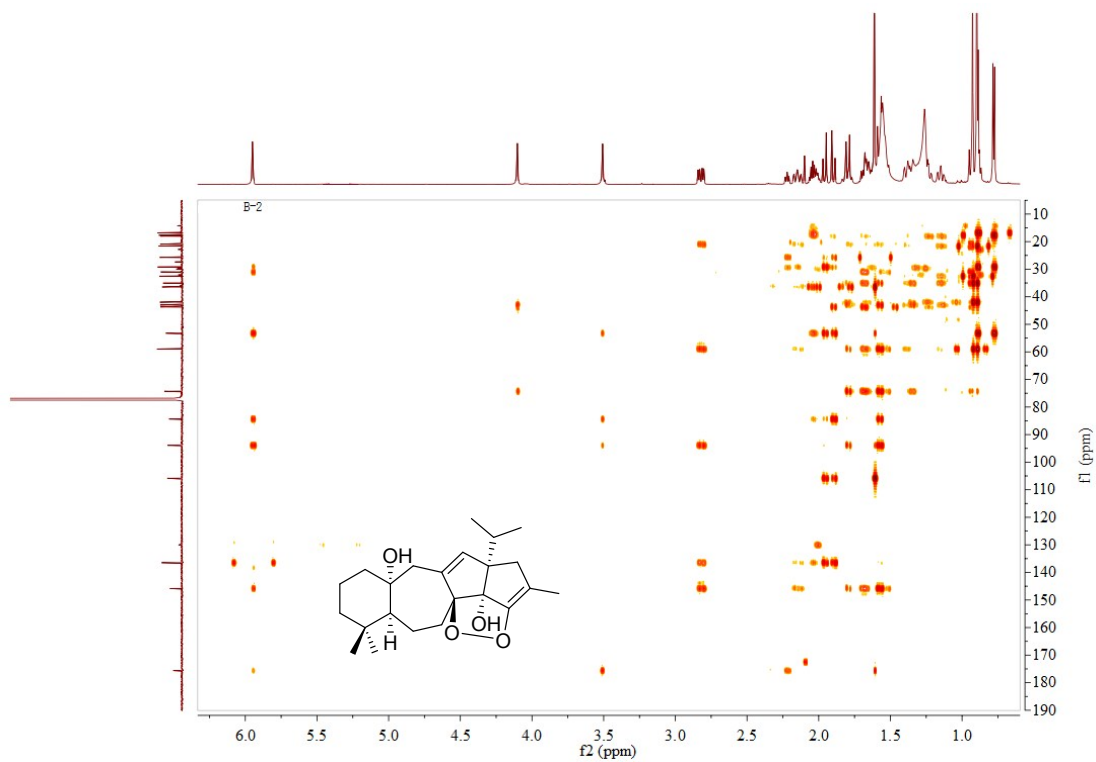


Fig. S8 HMBC spectrum of officinalin A (1) in CDCl₃

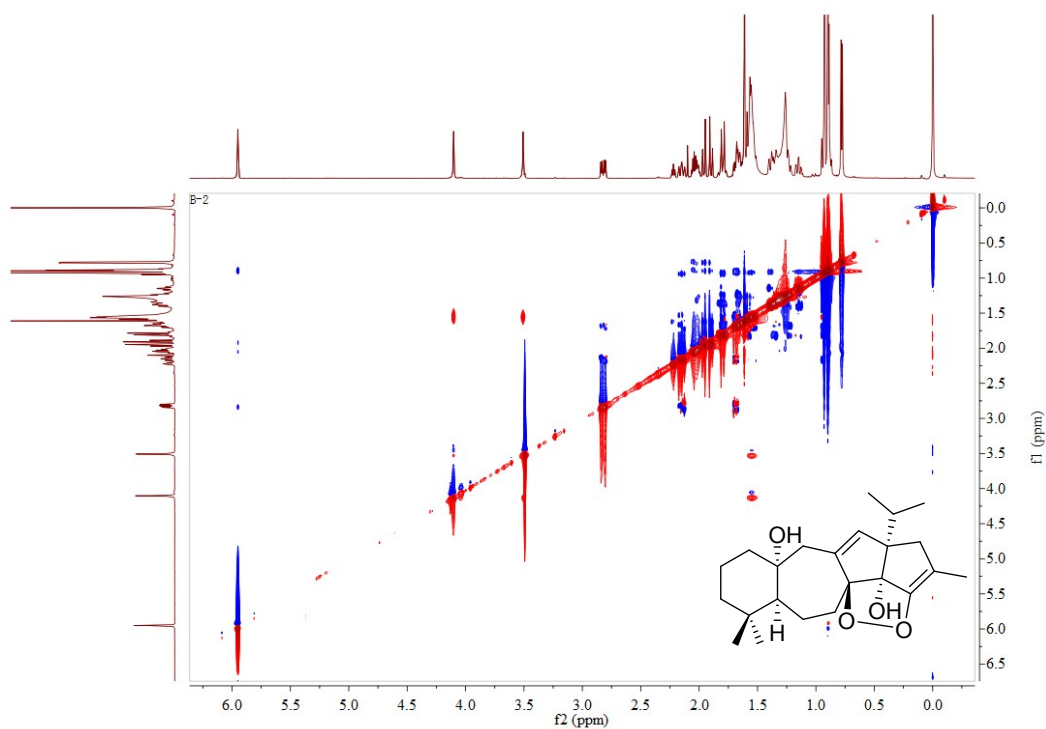


Fig. S9 ROESY spectrum of officinalin A (1) in CDCl₃

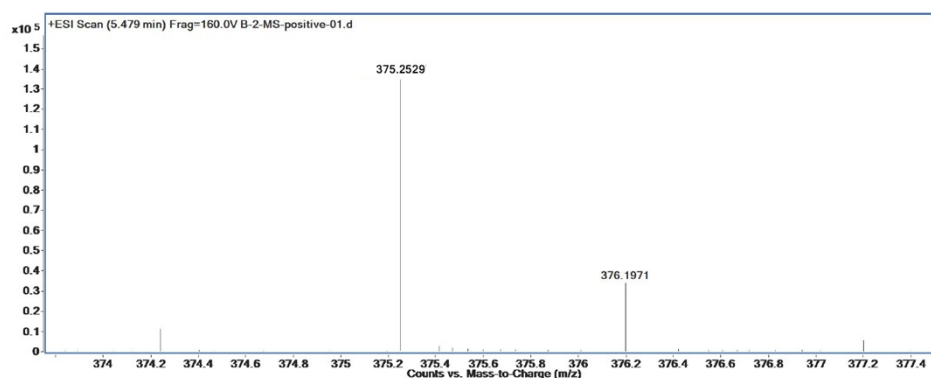
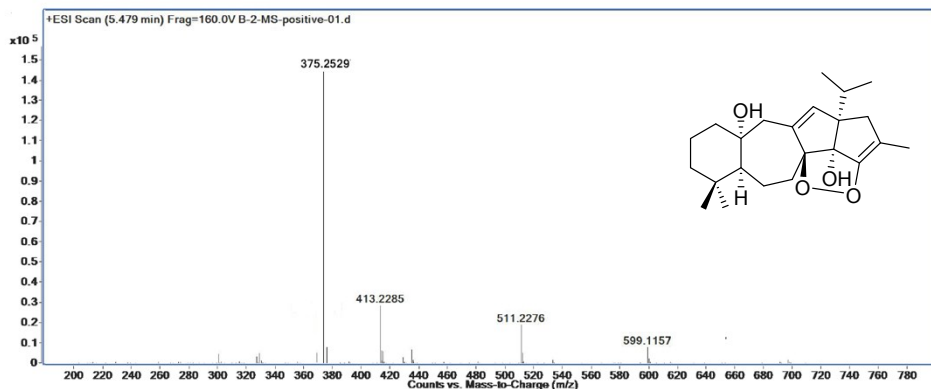
TCM-CPU HR-ESI-MS Display Report

Sample Name: B-2

Instrument: Agilent 6520B Q-TOF

Acq. Date: 01/19/2019

Operator: Administrator



Elemental Composition Calculator

Target m/z:	375.2529	Result type:	Positive ions	Species:	[M+H] ⁺
Elements:	C (0-80); H (0-120); O (0-30); N(0-10); Na (0-5)				
Ion Formula	Calculated m/z		PPM Error		
C ₂₃ H ₃₅ O ₄	375.2530		0.28		



Fig.S10 HRESIMS spectrum of officinalin A (1) in MeOH

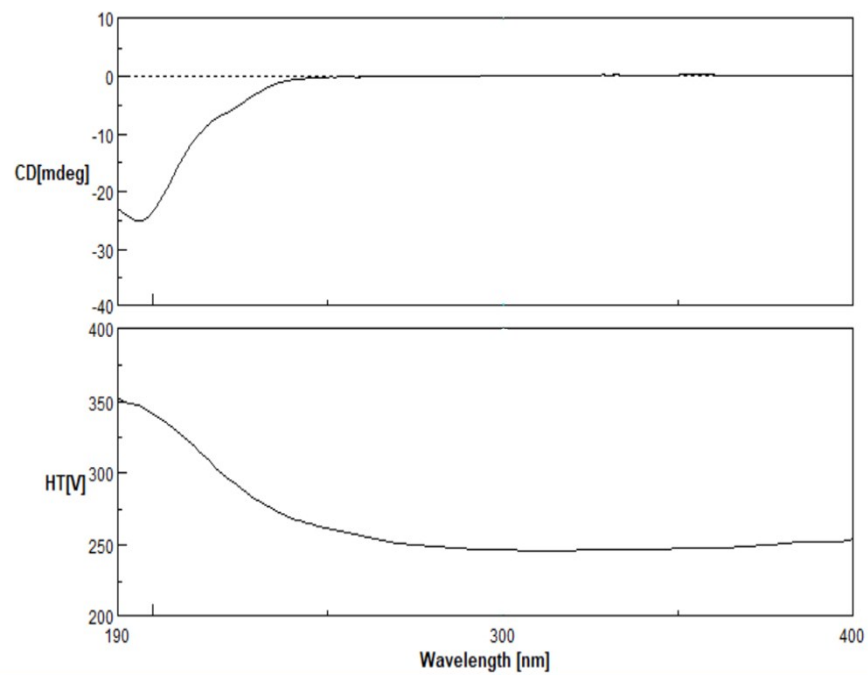


Fig. S11 CD spectrum of officinalin A (**1**) in MeCN

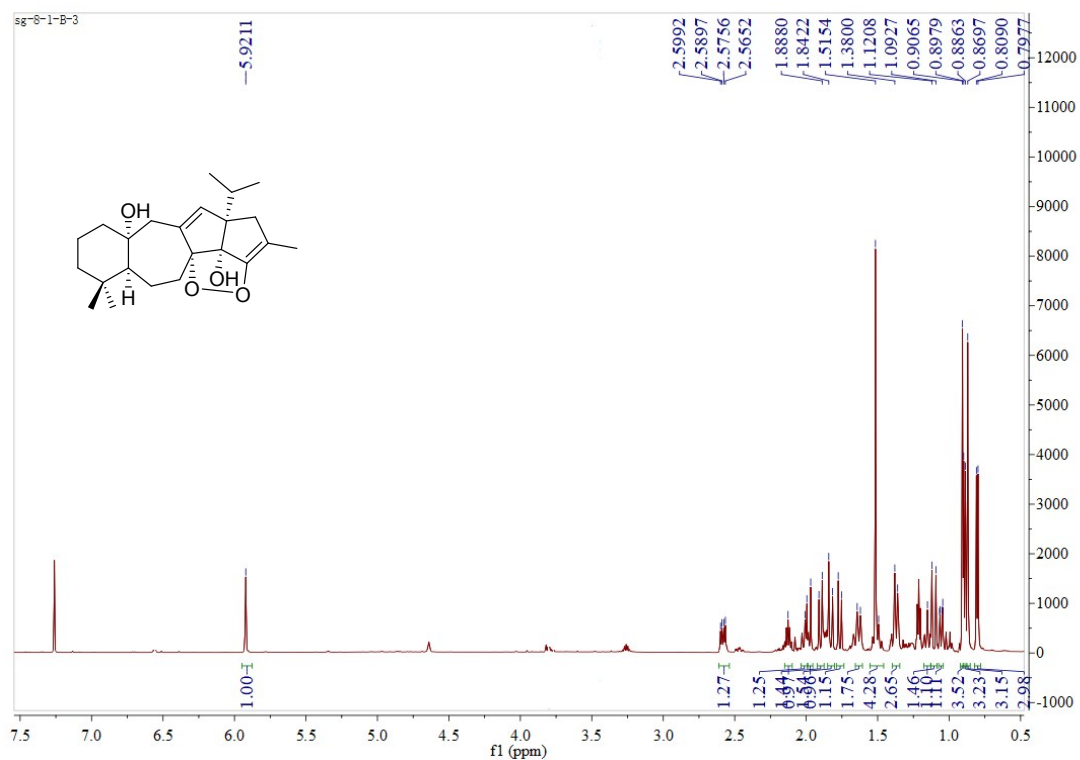


Fig. S12 ^1H NMR (600 MHz) spectrum of officinalin B (2) in CDCl_3

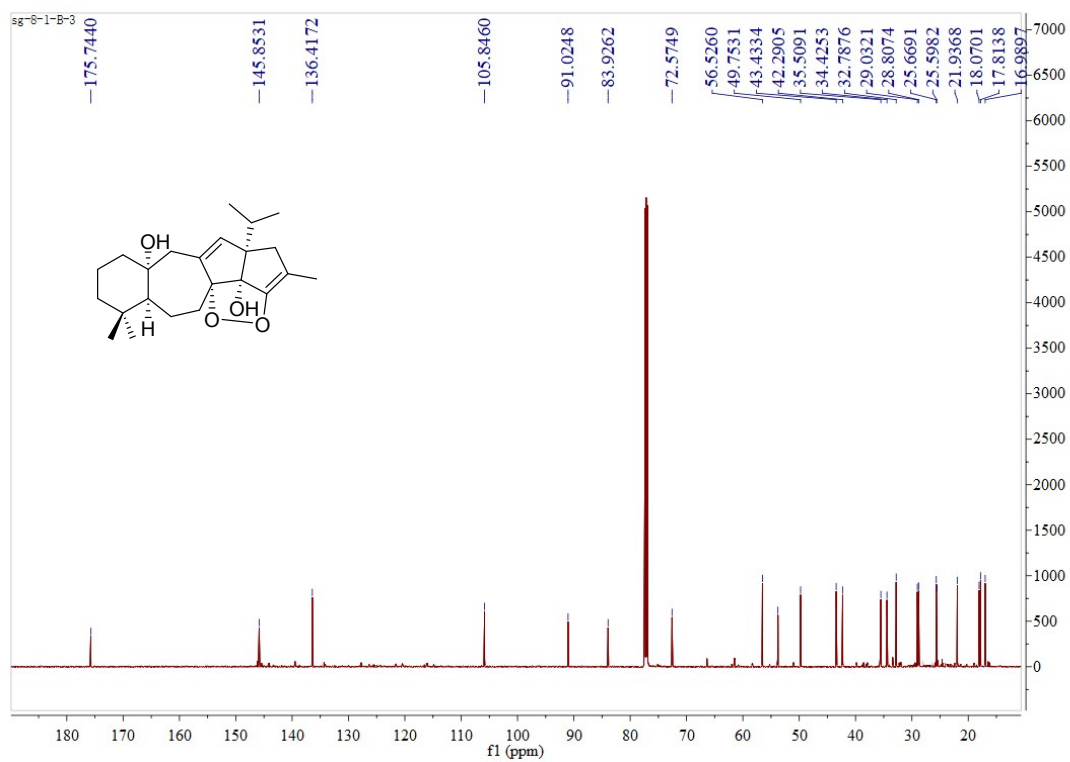


Fig. S13 ^{13}C NMR (150 MHz) spectrum of officinalin B (2) in CDCl_3

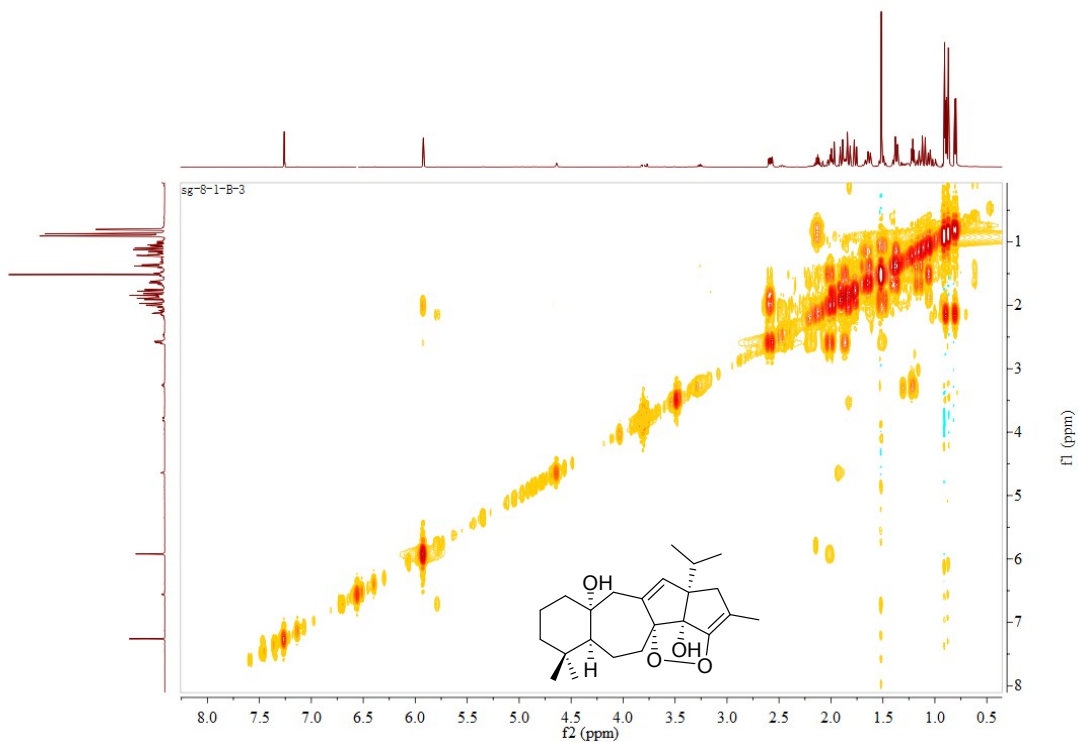


Fig. S14 ^1H - ^1H COSY spectrum of officinalin B (**2**) in CDCl_3

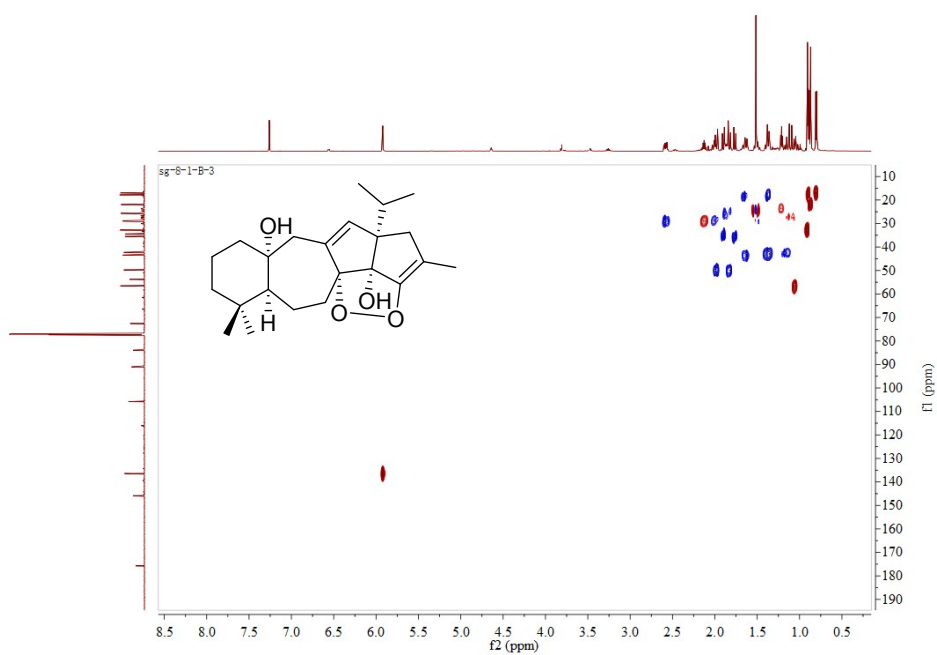
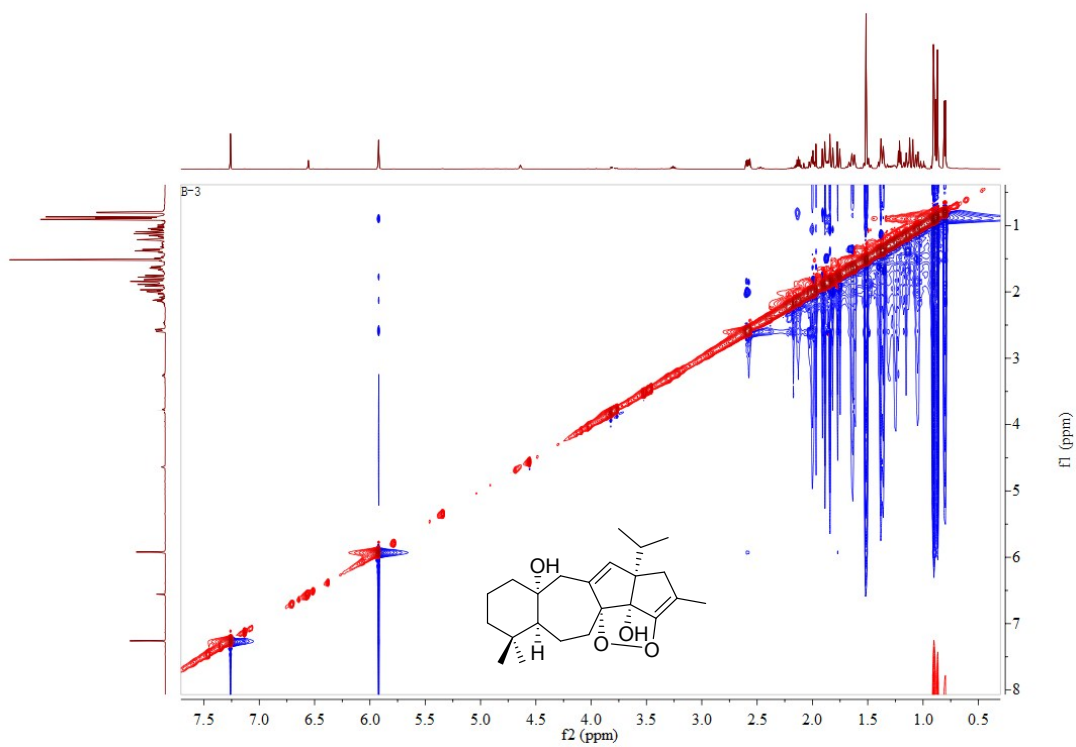
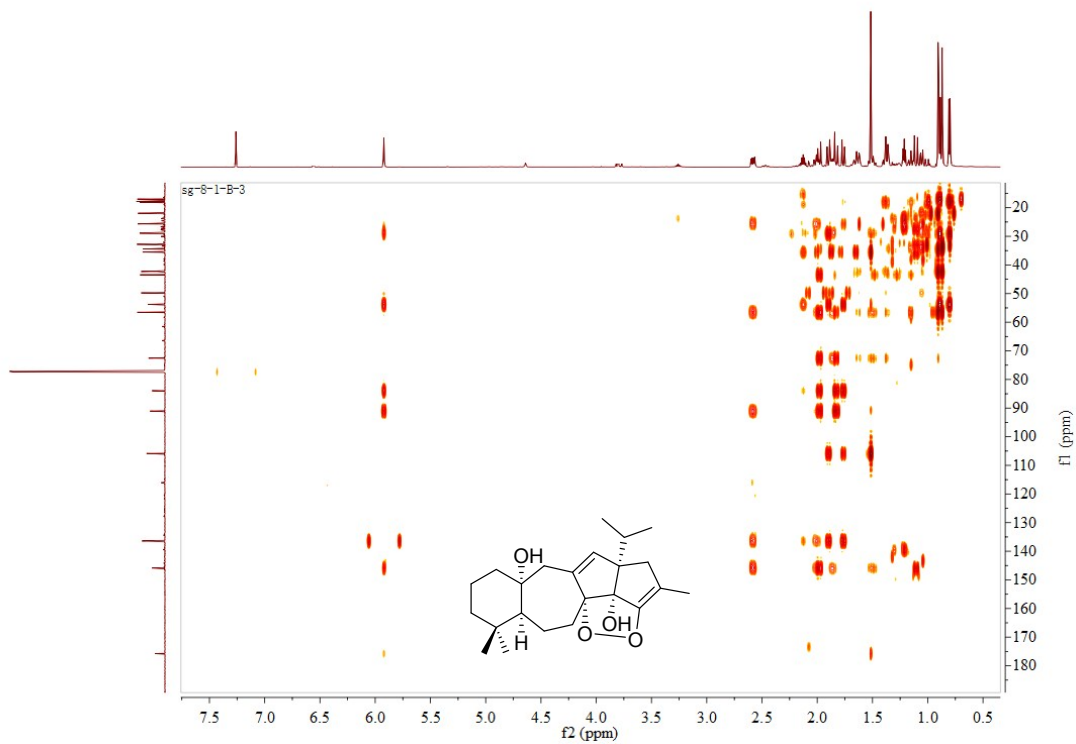


Fig. S15 HSQC spectrum of officinalin B (**2**) in CDCl_3



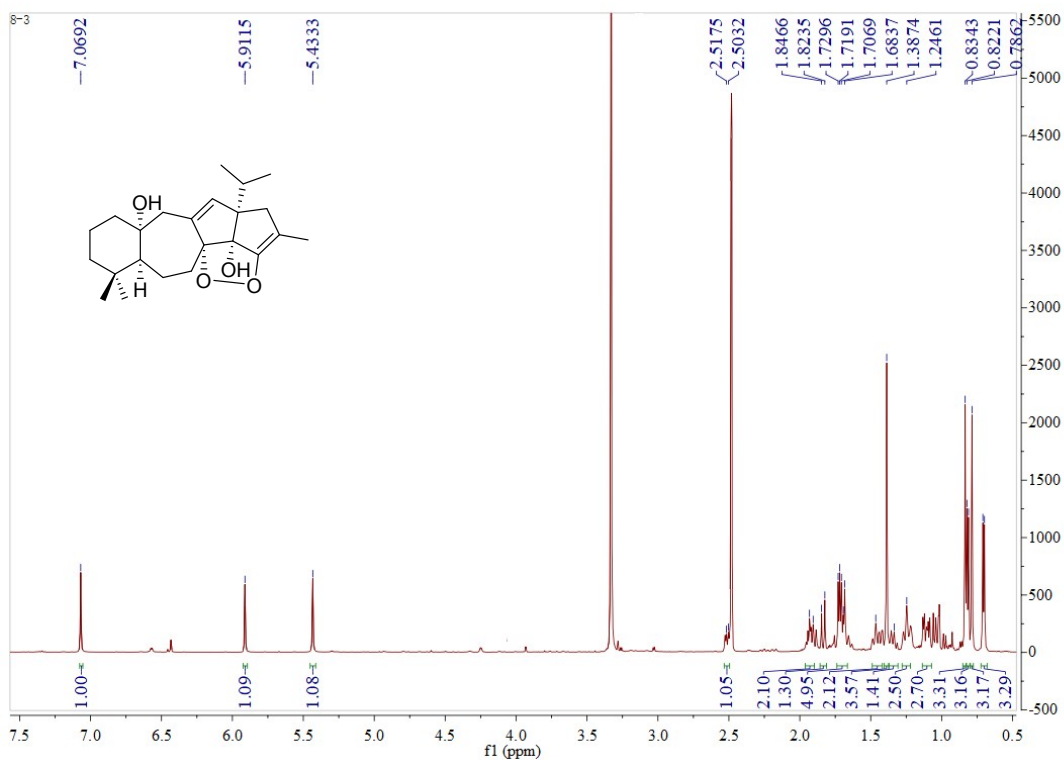


Fig. S18 ^1H NMR (600 MHz) spectrum of officinalin B (**2**) in $\text{DMSO-}d_6$

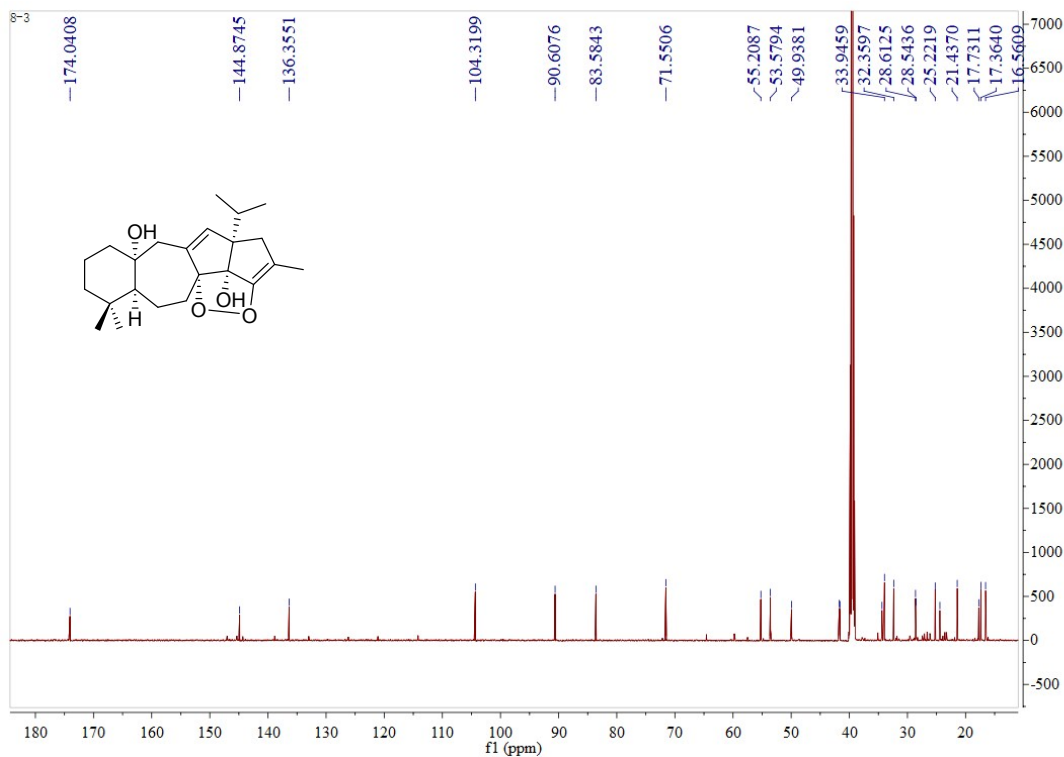


Fig. S19 ^{13}C NMR (150 MHz) spectrum of officinalin B (**2**) in $\text{DMSO-}d_6$

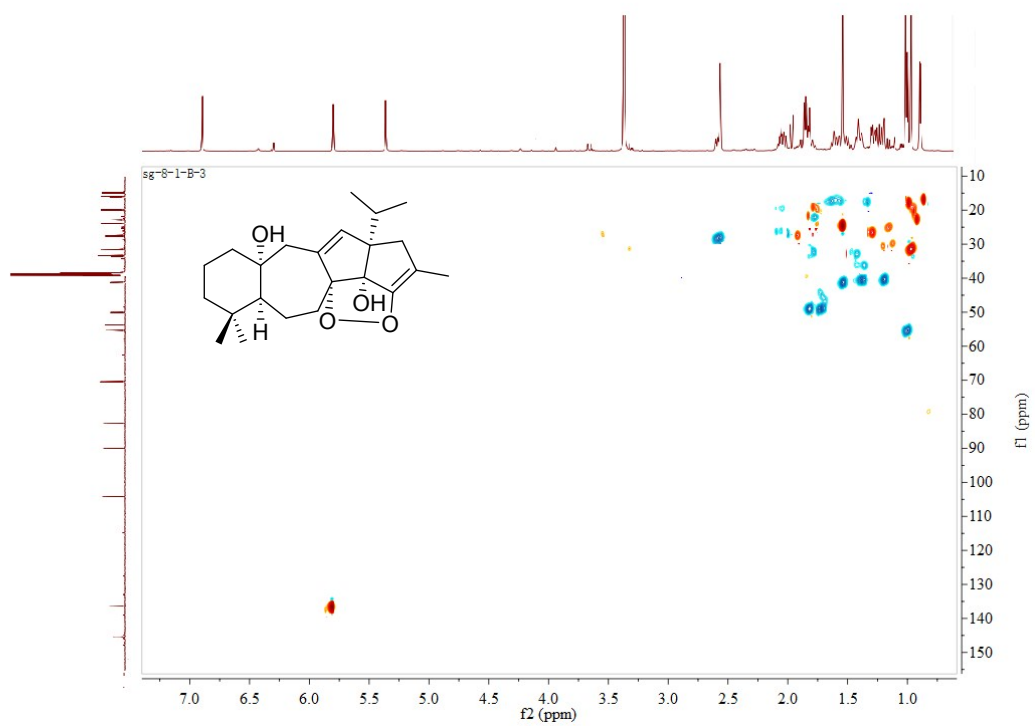


Fig. S20 HSQC spectrum of officinalin B (**2**) in DMSO- d_6

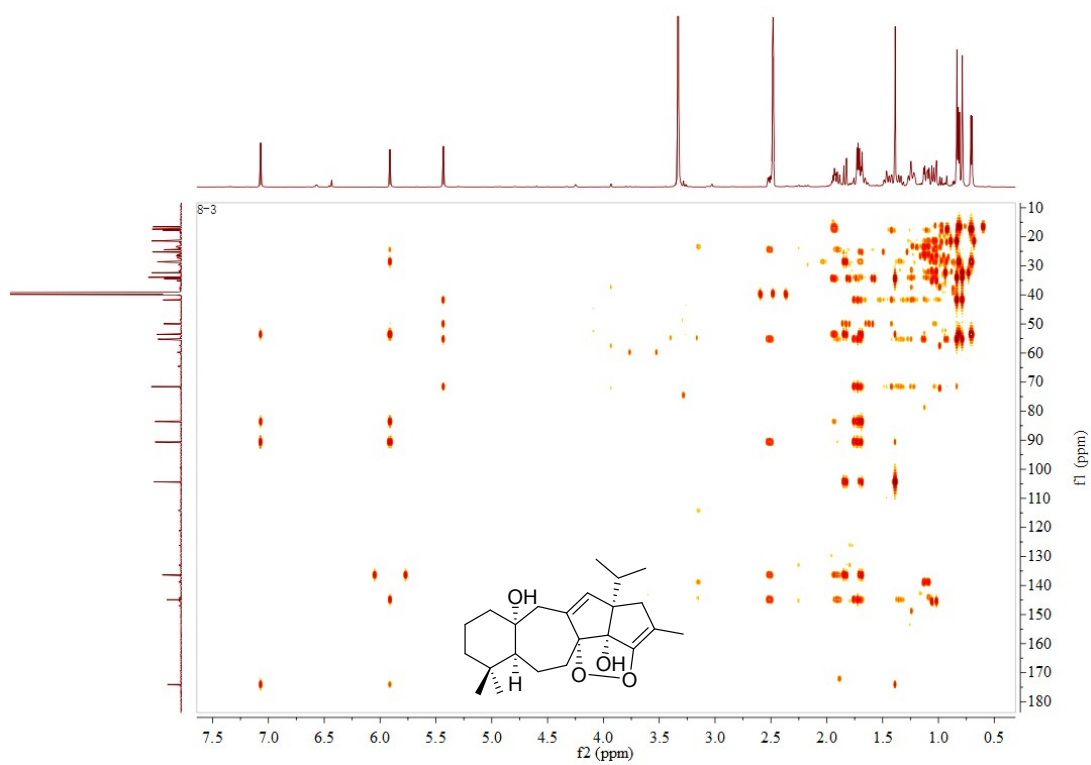


Fig. S21 HMBC spectrum of officinalin B (**2**) in DMSO- d_6

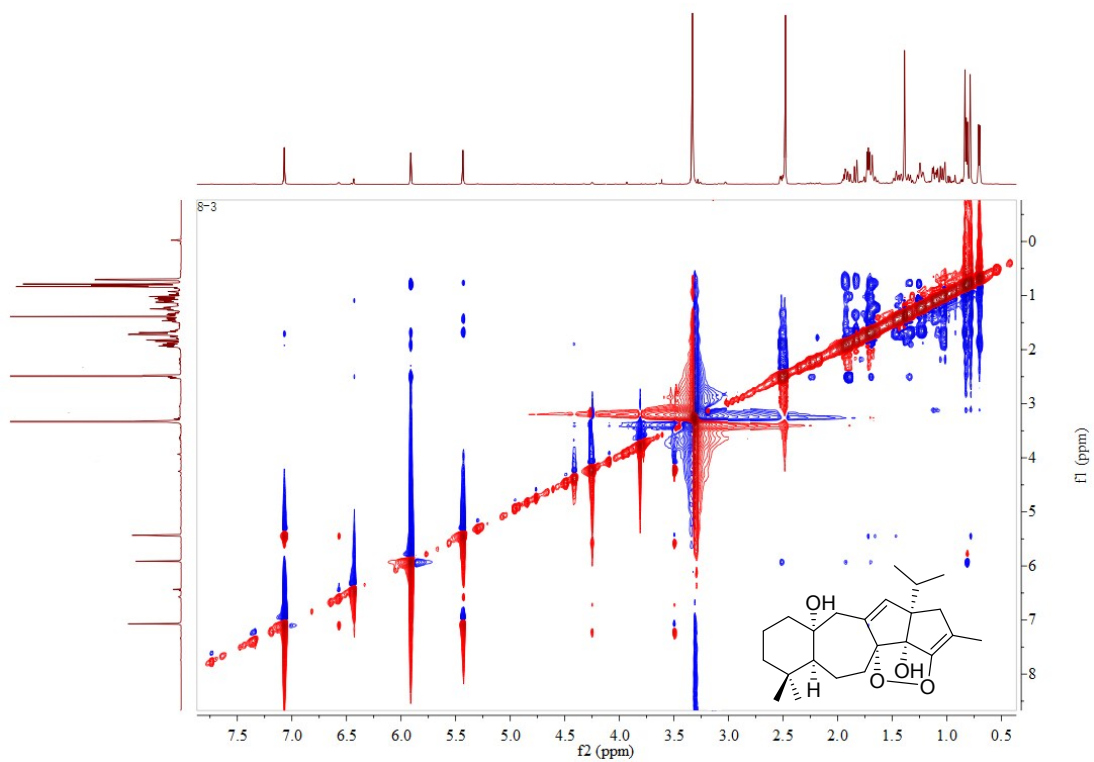


Fig. S22 ROESY spectrum of officinalin B (**2**) in DMSO-*d*₆

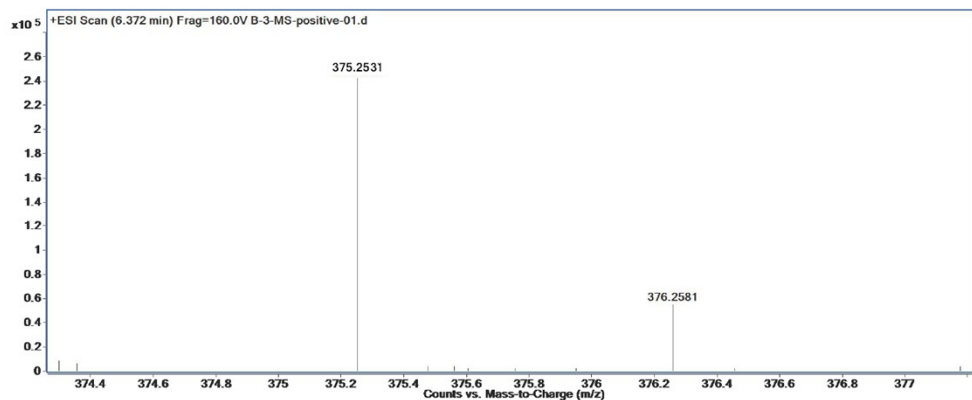
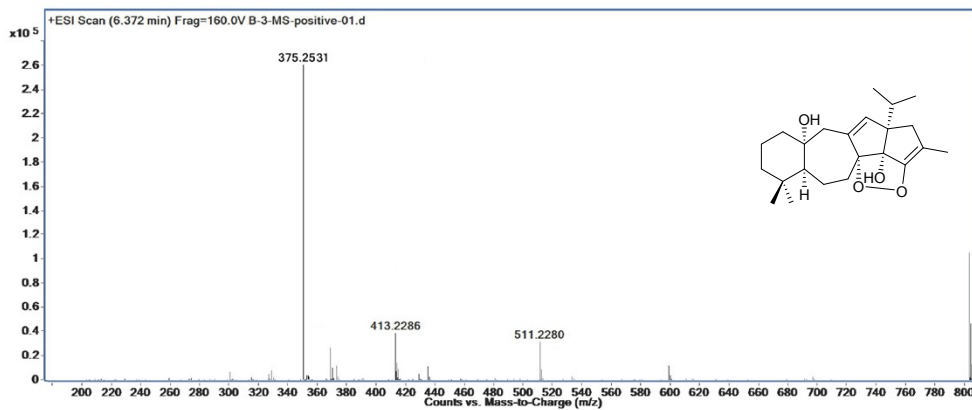
TCM-CPU HR-ESI-MS Display Report

Sample Name: B-3

Instrument: Agilent 6520B Q-TOF

Acq. Date: 01/19 /2019

Operator: Administrator



Elemental Composition Calculator

Target m/z:	375.2531	Result type:	Positive ions	Species:	[M+H] ⁺
Elements:	C (0-80); H (0-120); O (0-30); N(0-10); Na (0-5)				
Ion Formula	Calculated m/z		PPM Error		
C ₂₃ H ₃₅ O ₄	375.2530		-0.56		

 Agilent Technologies

Fig. S23 HRESIMS spectrum of officinalin B (2) in MeOH

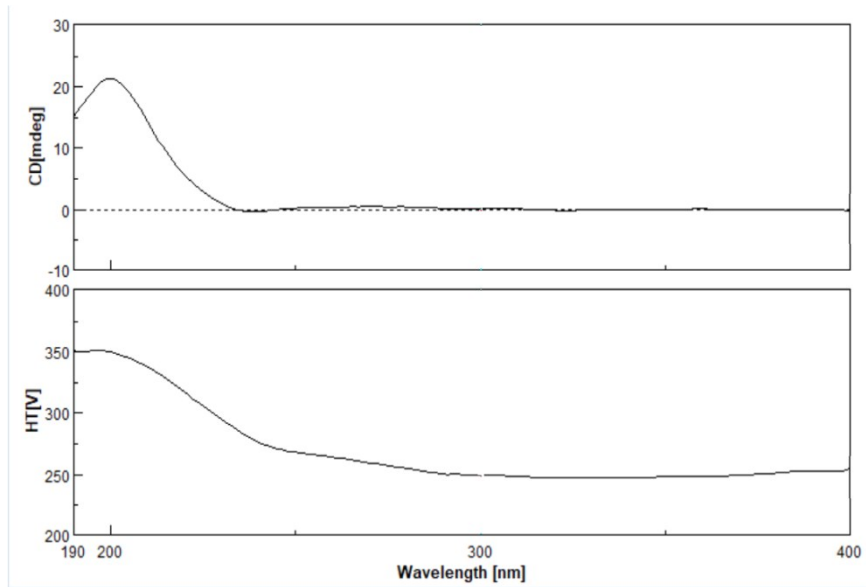


Fig. S24 CD spectrum of officinalin B (**2**) in MeCN

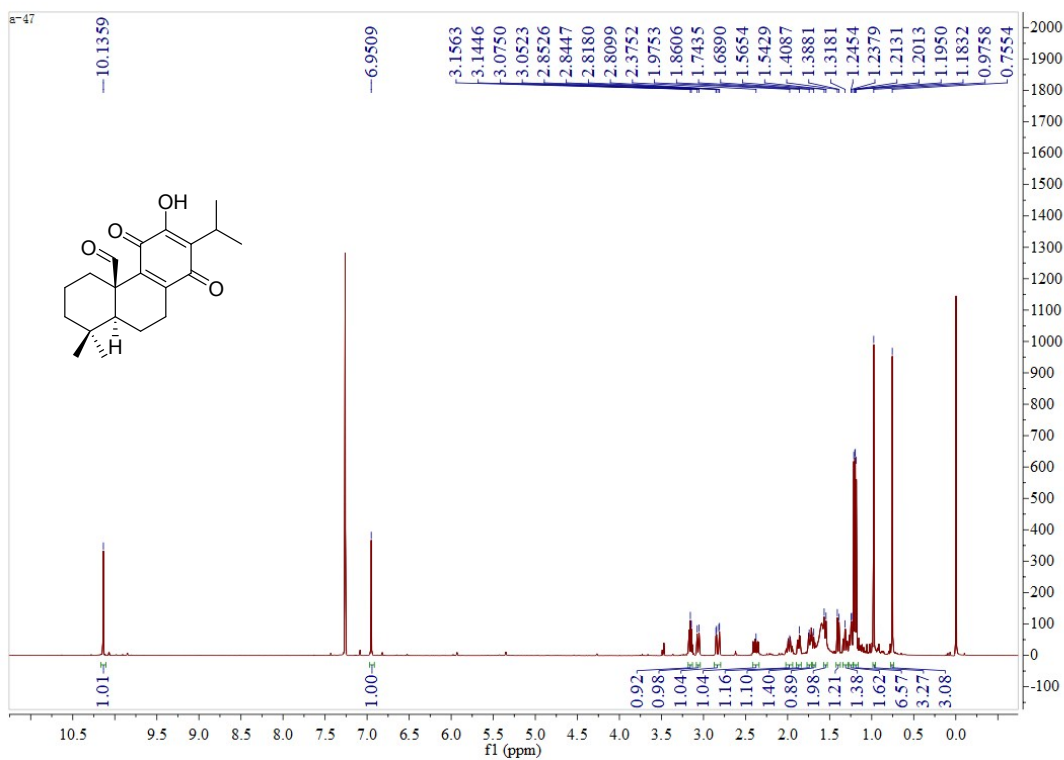


Fig. S25 ^1H NMR (600 MHz) spectrum of compound **3** in CDCl_3

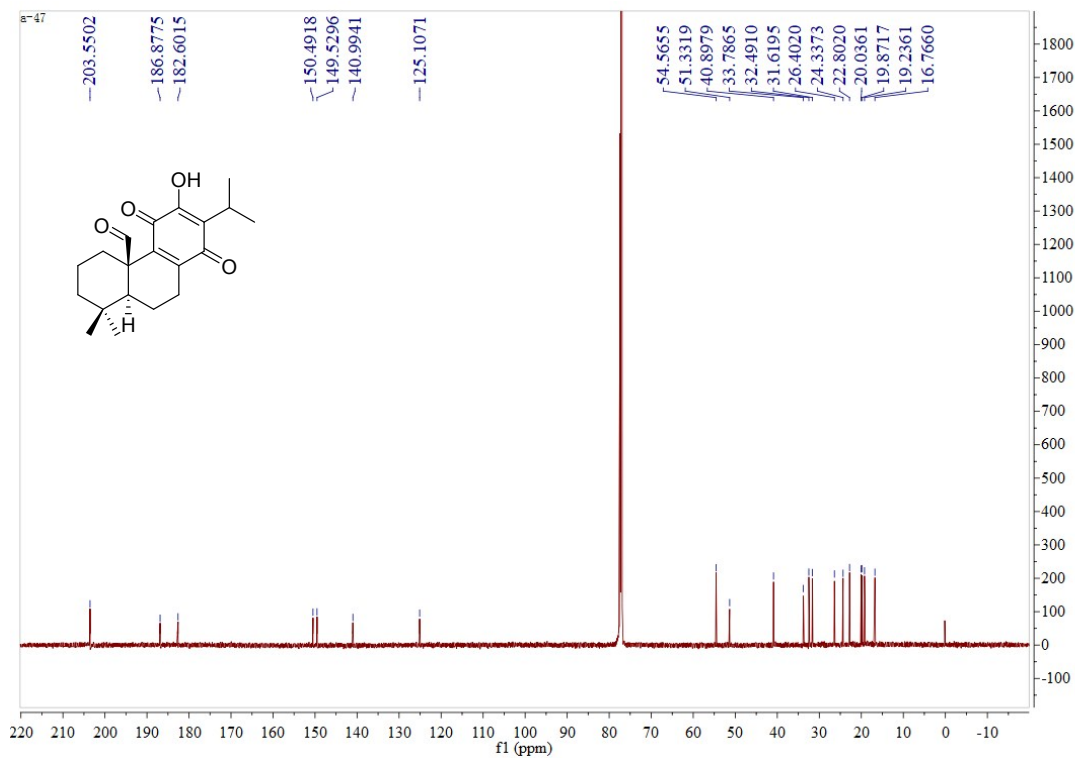


Fig. S26 ^{13}C NMR (150 MHz) spectrum of compound **3** in CDCl_3